Received November 19, 2021, accepted January 15, 2022, date of publication January 21, 2022, date of current version February 3, 2022.

*Digital Object Identifier 10.1109/ACCESS.2022.3145674*

# Methodology Based on Vector and Scalar Measurement of Traffic Channel Power Levels to Assess Maximum Exposure to Electromagnetic Radiation Generated by 5G NR Systems

**SARA ADDA[1], TOMMASO AURELI[2], SERGIO BASTONERO[3], STEFANO D'ELIA[4], DANIELE FRANCI[2], ENRICO GRILLO[2], MARCO DONALD MIGLIORE[5,6], (Senior Member, IEEE), NICOLA PASQUINO[7], (Senior Member, IEEE), SETTIMIO PAVONCELLO[2], FULVIO SCHETTINO[5,6], (Senior Member, IEEE), ANDREA SCHIAVONI[3], (Member, IEEE), RENATO SCOTTI[3], RICCARDO SUMAN[4], AND MATTIA VACCARONO[1]**

[1]Dipartimento Rischi Fisici e Tecnologici, Arpa Piemonte, 10015 Ivrea, Italy
[2]Agenzia per la Protezione Ambientale del Lazio (ARPA Lazio), 00172 Rome, Italy
[3]Telecom Italia SpA, 00165 Turin, Italy
[4]Vodafone Networks, Mobile Access Engineering, Vodafone Italia SpA, 10015 Ivrea, Italy
[5]Dipartimento di Ingegneria Elettrica e dell'Informazione "Maurizio Scarano" (DIEI) and ELEDIA Research Center (ELEDIA@UniCAS), University of Cassino and Southern Lazio, 03043 Cassino, Italy
[6]National Inter-University Consortium for Telecommunications (CNIT), 43124 Parma, Italy
[7]Dipartimento di Ingegneria Elettrica e delle Tecnologie dell'Informazione, Università degli Studi di Napoli Federico II, 80125 Napoli, Italy

Corresponding author: Nicola Pasquino (nicola.pasquino@unina.it)

This work was supported in part by the Ministry of Education, University and Research under Grant Dipartimenti di Eccellenza (2018–2022)

**ABSTRACT** Maximum-Power Extrapolation (MPE) for mobile telecommunication sources follows an established paradigm based on the identification and measurement of a channel that acts as a power reference. Prior to the 5G era, the role of reference channel has been played by always-on broadcast signals since they had the great advantage of being always transmitted at the maximum power level allowed for a generic signal channel. However, the beamforming implemented by 5G sources obliges us to rethink this approach. In fact, with beamforming the 5G source can transmit data traffic streams through a beam characterized by a much higher gain than the broadcast one. This implies that the detected power for traffic beams could be much higher than the corresponding power of broadcast beams. In this paper, a novel approach for 5G MPE procedure is presented, where the direct measurement of the received power of a traffic beam is used to assess the maximum exposure generated by a 5G system. An innovative specific experimental setup is also proposed, with the use of a User Equipment (UE) with the aim of forcing the traffic beam toward the measurement positions. In this way, it is possible to directly measure the power of each Resource Element (RE) transmitted by the traffic beam. As opposed to other MPE proposals for 5G, the discussed technique does not require any correction of the measured data since it relies only on the traffic beam pointing toward the measurement position, simplifying the overall MPE procedure and thus reducing the uncertainty of the MPE estimated field strength.

**INDEX TERMS** Radio frequency, electromagnetic fields, exposure assessment, massive MIMO, 5G, new radio, measurements, mobile communication, channel power, zero span, vector measurements.

## I. INTRODUCTION

5G represents a major technological leap over previous generations of cellular systems. The stringent specifications of 5G, that must meet the requirements not only of human-to-human communication but also those of human-to-machine and machine-to-machine, required the introduction of numerous technological innovations. However, such innovations, like the beamforming technique inherent to 5G New Radio (NR) antenna systems, have raised new questions about

The associate editor coordinating the review of this manuscript and approving it for publication was Eyuphan Bulut.

the assessment and measurement of human exposure to the electromagnetic radiation generated by the new radiation paradigm. Also, the characterization of Power Control systems that limit the radiated power when specific time-averaged exposure limits are being approached is a topic of interest when a multiple-beam coverage is used like in a 5G NR [1].

To clarify the new challenges that 5G presents in this field, we recall that the estimation of the human exposure levels to electromagnetic fields essentially requires two steps. In the first phase, a special procedure, named Maximum-Power Extrapolation (MPE), allows to estimate the maximum expected field level radiated by the Next Generation NodeB (gNB) at the measurement point. It should be emphasized that the value obtained by the MPE procedure is an unrealistic upper limit, since it assumes that all the resources of the communication system are assigned to a single user. In the second phase, the MPE value is multiplied by an appropriate correction factor that takes into account the stochastic nature of the problem in order to obtain a realistic value [2]–[10].

With reference to the first phase, the standard MPE approach up to now has been based on the identification of a constant power reference signal that is always present (i.e., ''always on''), under the condition that all these signals are transmitted with constant and maximum power at all times.

This condition is not totally fulfilled in 5G, because of a different approach to the managing of ''always on'' signals and because of beamforming. In particular, 5G uses an energy-efficient signaling strategy, limiting ''always on'' signals as much as possible. In fact, 5G contains all the fundamental information necessary to access the network in a signal structure highly concentrated in frequency, time and possibly space, called SS/PBCH Block (SSB).

In addition, 5G systems implement antenna solutions able to transmit user data on a different beam (named *traffic beam*) than the beam used to transmit the SSB channel (named *broadcast beam*). This approach is used both in sub-6 GHz active antennas and in mm-Wave band [11]. Since the traffic beam usually has a greater directivity than the broadcast one, there is a power increase factor with respect to the power level measured by SSB which must be taken into account in MPE.

The innovations introduced by 5G technology oblige to rethink and innovate the established paradigm of MPE procedure. Due to beamforming, 5G systems are characterized by dynamic, high-gain traffic beams focused towards the UE resulting in received power levels that may be much higher than the corresponding power of broadcast beams. For this reason, the definition of an effective MPE procedure for active antenna systems implementing beamforming is currently ongoing in International Electrotechnical Commission (IEC) TC106X, that is revising IEC 62232 standard [12] in order to define a method to take into account this power increase. The complexity of the experimental scenario suggests to shift towards a novel approach for MPE, based on the usage of traffic Physical Downlink Shared CHannel (PDSCH) as the maximum power reference for 5G systems [13].

This paper presents an innovative proposal for 5G MPE procedure based on direct measurement of the PDSCH power level using both Vector Signal Analyzer (VSA) and Spectrum Analyzer (SA). In addition, to address the issues introduced by beamforming, the procedure requires an original experimental setup based on the use of a UE, with the aim of forcing the 5G system to focus a high-gain traffic beam towards the point of interest, throughout the whole duration of the PDSCH power measurement. Experimental results collected at several 5G sites confirm the validity of the proposed method, providing an accurate validation of its effectiveness.

The paper is organized as follows: in Sect. II a review of the MPE procedure is given, while in Sect. III the measurement setup is presented. Experimental results are presented and discussed in Sect. IV: specific subsections are provided for each tested methodology, along with an overall comparison. Measurement procedures are thoroughly discussed in Appendix.

## II. THE MAXIMUM-POWER EXTRAPOLATION PROCEDURE

Although the experimental procedure for the assessment of human exposure to radio frequency (RF) electromagnetic fields is strongly dependent on the specific characteristics of the radio system, the methodologies adopted for getting the maximum received power in a measurement point - independently by the technology - are based on the identification of a *reference channel*. In order to be eligible to serve as a reference for the received power, a channel requires a time-constant transmitted power representing an upper bound for the allowed transmitted power of a generic channel of the radio system. Once the reference channel received power $P_{\mathrm{ref}}$ is measured, the extrapolated maximum power $P_{\mathrm{max}}$ that can be received in the measurement point can be obtained by eq. (1):

$$P_{\mathrm{max}} = K \cdot P_{\mathrm{ref}} \tag{1}$$

where $K$ is a technology-dependent constant.

Prior to 5G technology, the role of reference channel has been played by system-specific broadcast control channels — Broadcast Control CHannel (BCCH) for 2G [14], [15], Primary Common PIlot CHannel (P-CPICH) for 3G and Cell specific Reference Signal (CRS) for 4G — which had the great advantage to be always on and moderately easy to detect. For this reason, many early works about 5G electromagnetic field (EMF) assessment were based on the measurement of the power levels associated with the SSB [11], [13], [16]–[21]. Nevertheless, it soon became evident that the SSB power could not be representative of the maximum power level of data channel due to the beamforming mechanism.

The peculiar ability of the active antenna systems — widely used for 5G technology — to focus narrow, high-gain traffic beams to specific end-user directions implies that the PDSCH is received with a power level that could be several

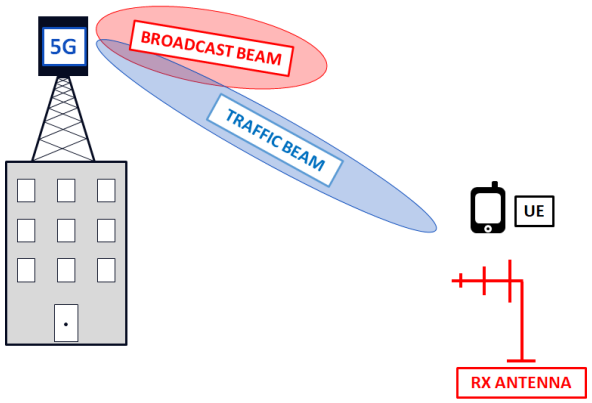


**FIGURE 1.** Measurement scenario.

order of magnitude higher than the broadcast control channels. This behavior implies, for signals generated by active antenna systems, that PDSCH power per Resource Element (RE) $P_{\text{PDSCH-RE}}$ can be assumed as an effective candidate for $P_{\text{ref}}$ for maximum power extrapolation just as long as the measurement is carried out while a traffic beam is pointing to the receiver antenna. This condition can be achieved by forcing a connection between the radio base station and a UE placed in the measurement point (Fig. 1).

Under this assumption, eq. (1) for 5G signals can be rewritten as:

$$P_{\text{max}} = N_{\text{sc}}(\mu, B) \cdot F_{\text{TDC}} \cdot P_{\text{PDSCH-RE,max}}, \qquad (2)$$

where:

- $N_{\text{sc}}(\mu, B)$ is the total number of sub-carriers, which depends on both the numerology $\mu$ and channel bandwidth $B$ of the incoming signal;
- $F_{\text{TDC}}$ is the Time-Division Duplexing (TDD) duty-cycle scale factor defined in [12];
- $P_{\text{PDSCH-RE,max}}$ is the maximum PDSCH received power per RE, according to the measurement scenario shown in Fig. 1.

Strictly speaking, the key step of the experimental methodology for the assessment of the maximum 5G received power is the on-field measurement of $P_{\text{PDSCH-RE,max}}$. In the following, two alternative methods for the assessment of $P_{\text{PDSCH-RE,max}}$ will be presented, based on code-domain and Zero Span (ZS) measurements.

## III. MEASUREMENT SET-UP AND PROCEDURE

Two types of experimental campaigns have been conducted, the first one under controlled laboratory conditions and the second one consisting of on-site measurements.

### A. CONTROLLED-ENVIRONMENT MEASUREMENT SETUP

In the controlled-environment experimental session, the following setup has been used:

- an Anritsu MG3710E Vector Signal Generator (VSG), equipped with IQproducer MX269913A software for sub-6GHz 5G signal generation;

**TABLE 1.** Controlled-environment signal configuration.

| | |
|---|---|
| Center frequency $f_c$ | 3700 MHz |
| Bandwidth $B$ | 80 MHz |
| Duplexing | TDD |
| Frame configuration | D-D-D-D-D-D-D-S-U-U |
| Special slot | 6:4:4 |
| $F_{\text{TDC}}$ | 0.743 |
| Numerology $\mu$ | 1 |
| Sub-carrier spacing $\Delta f$ | 30 kHz |
| Symbol duration | 33.3 µs |
| SSB center frequency | 3700 MHz |
| SSB allocation [22, §4] | Case C |
| SSBs per burst | 8 |
| SSB periodicity | 10 ms |
| Downlink traffic | full frame |

**TABLE 2.** Controlled environment measurement setup.

| Parameter | Requirement | Settings |
|---|---|---|
| Frequency | SSB center frequency | depends on operator |
| SweepTime (SWT) | $\geq$ SSB rep. period | 20, 33, 40 ms |
| Resolution Bandwidth (RBW) | $\leq$ SSB bandwidth | 1, 3, 5, 6 MHz |
| Video Bandiwidth (VBW) | $\geq 3 \cdot$ RBW | 50 MHz |
| Detector | RMS detector | RMS |
| Trigger | Periodic | SSB repetition period (20 ms) |
| Trace | power averaging (full-traffic) | AVG |

- a Rohde & Schwarz (R&S) FSVA 3030 VSA, equipped with the dedicated 5G demodulation software.

The 5G VSG was connected directly to the VSA through a coaxial cable. The main characteristics of the generated signals are summarized in Tab. 1.

The instruments configuration for measurements in the controlled environment is reported in Tab. 2.

### B. ON-SITE MEASUREMENT SETUP

For the on-site measurements, three operation sites located in Ivrea, Rome and Turin were chosen where 5G NR gNBs by two different vendors were active. Fig. 2 shows that each site allowed a full Line-of-Sight (LOS) propagation. The configuration of the signal sources is shown in Tab. 3. The following list shows the type of measurements and the instrumentation for each site:

Ivrea Measurements were performed with a Keysight N9020A VSA, connected through a coaxial cable to a Schwarzbeck SBA 9112 antenna. The analyzer was set in ZS mode at the SSB center frequency, and Max-hold (MH), Average (AVG) and min-hold (mh) traces were acquired.

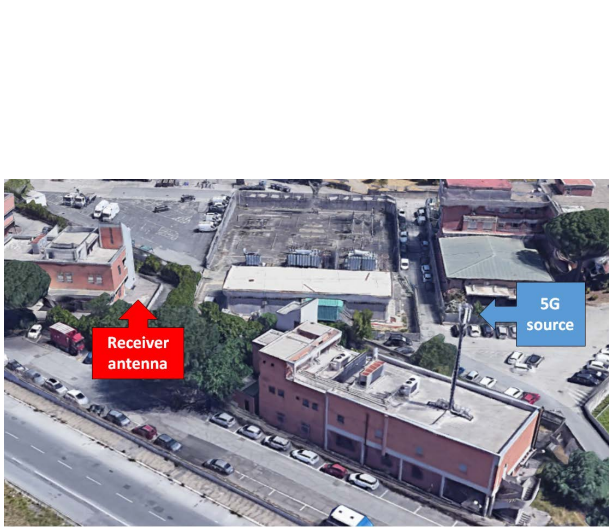


(a) Overview of measurement site in Rome.

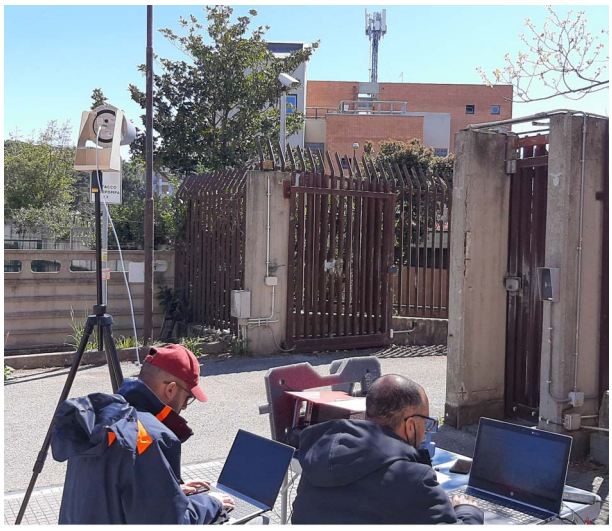

(b) 5G antenna viewed from the measurement site in Rome.

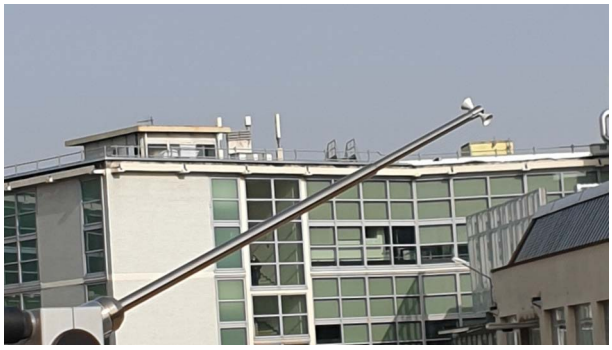

(c) Overview of measurement site in Ivrea.


(d) Overview of measurement site in Turin.

**FIGURE 2.** Measurement sites.

**TABLE 3.** On-site measurement sources configuration.

| | Ivrea | Rome | Turin |
|---|---|---|---|
| Vendor | Vendor 1 | Vendor 2 | Vendor 2 |
| Center frequency $f_c$ | 3680 MHz | 3759.99 MHz | 3759.99 MHz |
| Bandwidth $B$ | 80 MHz | 80 MHz | 80 MHz |
| Duplexing | TDD | TDD | TDD |
| Frame configuration | D-D-D-D-D-D-D-S-U-U | D-D-D-S-U-U-D-D-D-D | D-D-D-S-U-U-D-D-D-D |
| Special slot | 5:2:5:2 (SS 54) | 6:4:4 | 6:4:4 |
| $F_{\text{TDC}}$ | 0.743 | 0.743 | 0.743 |
| Numerology $\mu$ | 1 | 1 | 1 |
| Subcarrier spacing $\Delta f$ | 30 kHz | 30 kHz | 30 kHz |
| Symbol duration | 33.3 µs | 33.3 µs | 33.3 µs |
| SSB center frequency | 3679.68 MHz | 3731.52 MHz | 3731.52 MHz |
| SSB allocation [22, §4] | Case C | Case B | Case B |
| SSBs per burst | 8 | 1 | 1 |
| SSB periodicity | 20 ms | 20 ms | 20 ms |

Turin Measurements were run with a Keysight N9020A VSA and a R&S FSW connected to the same Schwarzbeck SBA 9112 antenna through a power splitter. The VSA was set in ZS mode at the SSB center frequency, and MH, AVG and mh traces were acquired, while the FSW was used to demodulate the acquired frame.

Rome Measurements were run with a R&S FSVA 3030 VSA connected to an R&S HL050 log-periodic antenna through a coaxial cable. Both vector analysis of the

**TABLE 4. Scalar measurement setup.**

| Parameter | Requirement | Settings |
|---|---|---|
| Frequency | SSB center frequency | depends on operator |
| SweepTime (SWT) | $\geq$ SSB rep. period | 20, 33, 40 ms |
| Resolution Bandwidth (RBW) | $\leq$ SSB bandwidth | 1, 3, 5, 6 MHz |
| Video Bandiwidth (VBW) | $\geq 3 \cdot$ RBW | 50 MHz |
| Detector | RMS detector | RMS |
| Trigger | Periodic | SSB repetition period (20 ms) |
| Trace | power averaging (full-traffic) | AVG |

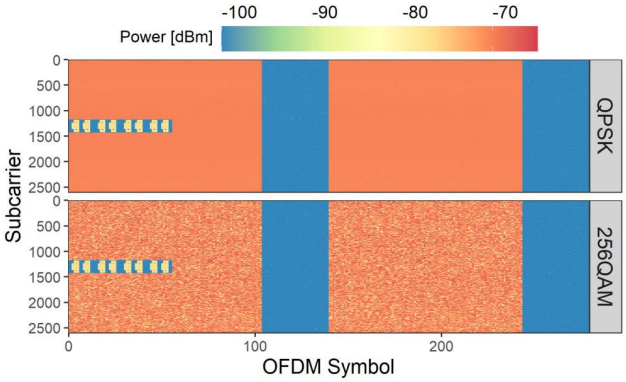


**FIGURE 3. Spectrograms of constant (QPSK) and non-constant (256QAM) amplitude modulation schemes of the PDSCH.**

demodulated 5G frame and ZS measurements were carried out. In addition, Channel Power (CP) measurements were used as a reference value for maximum power.

The instruments configuration for scalar measurements is reported in Tab. 4.

## IV. EXPERIMENTAL RESULTS

### A. CONTROLLED-ENVIRONMENT MEASUREMENTS

Preliminary measurements in a controlled environment were run to refine the procedure to be used during on-site measurements. Namely, the focus was to determine the effect of the modulation of the PDSCH on the demodulated power, considering both constant (QPSK) and non-constant (256QAM) amplitude modulations. Spectrograms in Fig. 3 show a full 10 ms frame when the two modulations are applied. They have been obtained by demodulating the signal received by the R&S FSVA 3030 VSA.

At first, let us consider the PDSCH signal with a QPSK modulation. As we can see in the top strip of Fig. 4, the effect is that there is a constant-power signal at the receiver input. As a matter of fact, the experimental *pdf* of the normalized power is very dense about the mean, and symmetric.

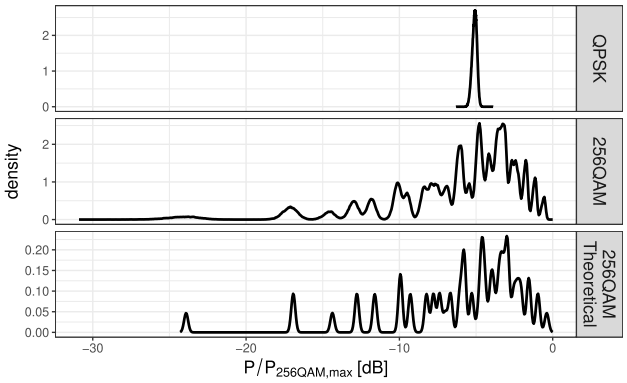


**FIGURE 4. Comparison of normalized power densities for actual QPSK and 256QAM (top and center strip), and theoretical 256QAM (bottom strip) PDSCH REs modulated signal.**

**TABLE 5. PDSCH statistics from Figs. 3 and 4.**

| Source | modulation | $\tilde{x}$ | $\bar{x}$ | $\Delta(\tilde{x},\bar{x})$ [dB] |
|---|---|---|---|---|
| | | [dBm] | | |
| Generator (actual – Fig. 3) | QPSK | -70.17 | -70.18 | 0.01 |
| | 256QAM | -70.02 | -71.36 | **1.34** |
| | | [dB] | | |
| Theoretical (normalized – Fig. 4) | 256QAM | -4.61 | -6.03 | **1.42** |

Then, let us consider the PDSCH with a 256QAM modulation. The center and bottom strips in Fig. 4 show the experimental and theoretical *pdf*s of the normalized power of the REs of that channel at the receiver input. As expected, the figure shows a large power spread, that is typical of the high-cardinality constellations adopted for payload data transmission, where many symbols of different amplitudes are used.

The observations above suggest a statistical approach to the evaluation of the power associated to the PDSCH, whose potential estimates are the median $\tilde{x}$ and mean $\bar{x}$ of the PDSCH REs received power. In the following, both estimates will be considered, and it will be shown that, in all the experimental cases considered for on-site measurements, they return compatible results when used in the MPE procedure.

Tab. 5 lists the values of $\tilde{x}$ and $\bar{x}$ from the actual QPSK- and 256QAM-modulated signals generated by the VSG and for the normalized theoretical 256QAM-modulated signal. We have also reported the difference $\Delta(\tilde{x},\bar{x})$ in dB of the two quantities. As expected, the QPSK modulation returns a substantially equal mean and median ($\Delta(\tilde{x},\bar{x}) \simeq 0$), while the 256QAM modulation results in distance between the two statistics that is almost the same for the actual and theoretical signal, which is consistent with the strong overlap of the two distributions in Fig. 4.

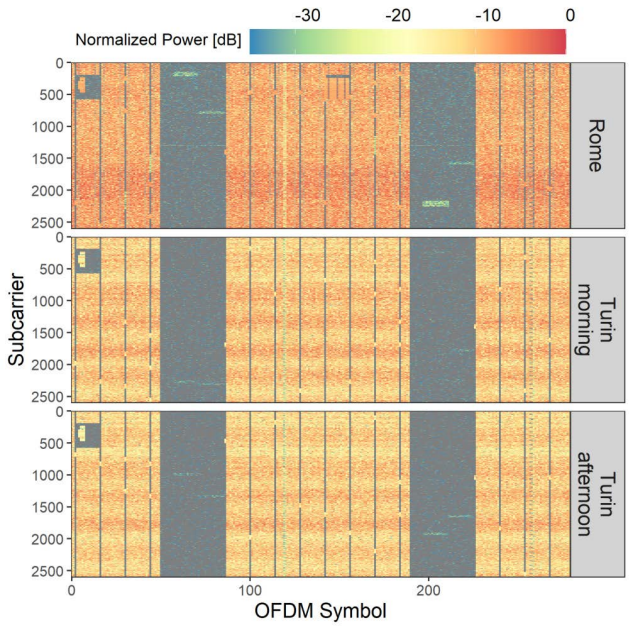


**FIGURE 5.** Normalized power spectrograms of signals generated at the three different sites.

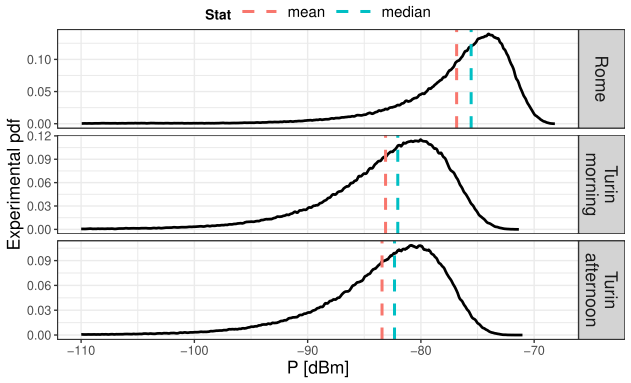


**FIGURE 6.** Experimental PDSCH REs *pdf*s at the three different sites.

### B. ON-SITE MEASUREMENTS: VECTOR APPROACH

The vector measurement approach for the evaluation of $P_{\text{PDSCH-RE,max}}$ has been applied to the measurement sites located in Rome and Turin (Fig. 2).

For both sites, the 5G radio frame has been demodulated to obtain a complete symbol per carrier grid with the received power of each RE. Measurements were run according to the experimental setup shown in Fig. 1, i.e., forcing the traffic with a UE to obtain a full-loaded frame. The radio frames acquired are shown by the spectrograms in Fig. 5, confirming that the connection between the UE and the gNB was very effective in inducing a complete PDSCH allocation within the frame at all measurement sites, although a fluctuation of the average power of the REs along the frequency axis can be observed. Measurements in Turin were run both in the morning and afternoon to check for repeatability, i.e., to make sure that no significant variation had occurred in either the source or the propagation channel over time.

**TABLE 6.** Sample statistics from Fig. 6.

| Site | $\tilde{x}$ | $\bar{x}$ | $\Delta(\tilde{x},\bar{x})$ | Sk | Ku |
|---|---|---|---|---|---|
| | [dBm] | | [dB] | | |
| Rome | −75.56 | −76.84 | **1.28** | −2.49 | 13.60 |
| Turin morning | −82.04 | −83.12 | **1.08** | −1.51 | 7.28 |
| Turin afternoon | −82.33 | −83.43 | **1.10** | −1.49 | 7.03 |
| | [pW] | | | | |
| Rome | 27.77 | 31.46 | | 0.86 | 3.61 |
| Turin morning | 6.25 | 8.41 | | 1.57 | 6.23 |
| Turin afternoon | 5.85 | 7.80 | | 1.54 | 6.15 |

As discussed in Sect. IV-A, the usage of 256QAM modulation for the PDSCH implies that the expected received power distribution of the associated REs is characterized by a large spread, due to the high crest factor of such a high-order modulation, unlike a constant-amplitude modulation like QPSK. Fig. 6 shows the *pdf* of the power of the PDSCH REs for the radio frames acquired both in Rome and Turin, with vertical dashed lines representing the mean (red) and median (green) value for each distribution. The presence of a large spread is confirmed, with the *pdf* typically spanning slightly more than the 30 dB interval that characterizes the 256QAM modulation in Fig. 4. The different smoothness can be explained by the fading, scheduling and boundary propagation conditions. The most relevant statistics of the distributions shown in Fig. 6 are listed in Tab. 6, where $\tilde{x}$ is the median and $\bar{x}$ is the mean. Focusing on the distance $\Delta(\tilde{x},\bar{x})$ between the dBm values of $\tilde{x}$ and $\bar{x}$, we can notice that its value is virtually that same for both measurements in Turin, possibly implying that the propagation channel has kept pretty stable during the day. Also, we can see that, on average, Turin has a smaller $\Delta(\tilde{x},\bar{x})$ than Rome.

The extrapolated maximum power $P_{\text{max}}$ has been assessed according to eq. (2) using both the median and mean as estimates for $P_{\text{PDSCH-RE,max}}$. A CP measurement (Fig. 7) has also been performed during the full-loaded frame condition as a reference for the expected $P_{\text{max}}$ value. An overall comparison between the extrapolated and reference $P_{\text{max}}$ value is presented in Tab. 7 with 95% ($k = 2$) expanded uncertainty. Results show that in each measurement site $\tilde{x}$ and $\bar{x}$ return extrapolated values that are compatible with the $P_{\text{CP}}$ reference value, confirming the results reported in [23] regarding the effectiveness of the proposed vector approach.

### C. ON-SITE MEASUREMENTS: SCALAR APPROACH

MPE from scalar measurements was obtained from ZS acquisitions in AVG mode and RMS detector, each consisting of the average of $n = 100$ traces.


**FIGURE 7.** CP measurement in Rome in download full-loaded frame condition.

**TABLE 7.** Comparison of $P_{\max}$ obtained through extrapolated ($P_{\text{MPE}}$) and reference ($P_{\text{CP}}$) values.

| Site | $P_{\text{MPE}}$ (median) | $P_{\text{MPE}}$ (mean) [nW] | $P_{\text{CP}}$ |
|---|---|---|---|
| Rome | $53.7 \pm 7.3$ | $60.9 \pm 8.3$ | $57.3 \pm 5.1$ |
| Turin morning | $12.1 \pm 2.5$ | $16.3 \pm 3.2$ | $12.2 \pm 2.4$ |
| Turin afternoon | $11.3 \pm 2.3$ | $15.1 \pm 3.0$ | $12.3 \pm 2.5$ |

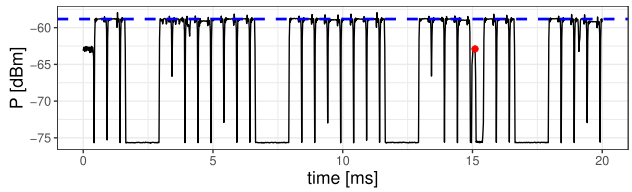


(a) Sample zero-span trace for AVG mode.

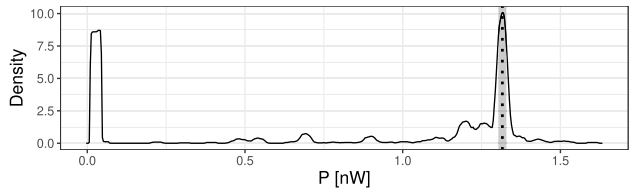


(b) Power density and modal value of traffic slots.

**FIGURE 8.** Zero-span trace and experimental density.

The reason for using the AVG mode is that while MH-mode acquisitions easily capture the full-frame condition required for the assessment of $P_{\text{PDSCH-RE,max}}$, they also detect the peak value of the power of the PDSCH REs $P_{\text{PDSCH-RE}}$ (i.e., the right tail of the distributions in Fig. 6) that could be not fully representative for MPE due to modulation and propagation conditions. A better representation of $P_{\text{PDSCH-RE}}$ can be obtained by using acquisitions averaged over a sufficiently extended time interval, thus minimizing the possibility of power overestimation.

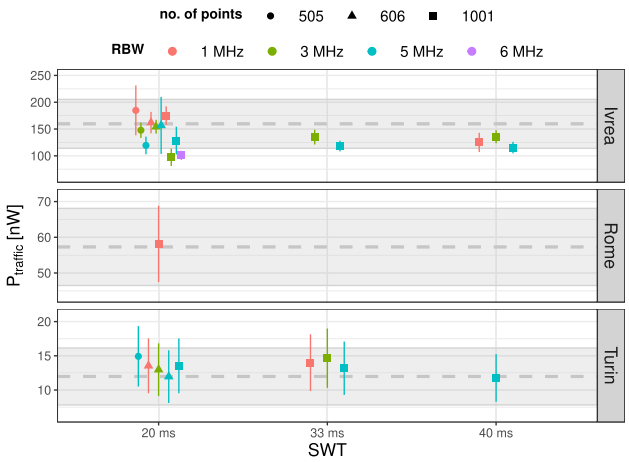


**FIGURE 9.** Comparison between MPE from ZS and CP measurements.

A sample of a ZS AVG trace is shown in Fig. 8a, where the red dot indicates the position of the SSB. After converting from dBm to nW, the power kernel density estimate was obtained through the `density()` function available in the `stats` library of the `R` language [24], using a rectangular kernel with a `binwidth` equal to 0.05 (see Fig. 8b). From the experimental density, the mode $x_{\text{mo}}$ of the traffic slots (indicated by the shadowed dotted line in Fig. 8b and, in log units, by the horizontal dashed blue line in Fig. 8a) was extracted. The use of $x_{\text{mo}}$ makes the procedure robust against transient power reductions, under the hypothesis that the most frequent value and the maximum received power are the same.

To obtain the estimate of the MPE power $P_{\text{traffic}}$ from $x_{\text{mo}}$, the following formula can been applied:

$$P_{\text{traffic}} = \frac{N_{\text{sc}} \cdot \Delta f}{\text{NBW}} \cdot x_{\text{mo}} \cdot F_{\text{TDC}}, \tag{3}$$

where $\Delta f = 30$ kHz is the sub-carrier frequency spacing for $\mu = 1$, and NBW is the noise bandwidth. Various configurations of the measurement equipment were tested at the sites shown in Fig. 2 and described in Tab. 3 to assess the effect on measurement results. The following factors and corresponding levels have been explored: SWT $=$ 20, 33, 40 ms, RBW $=$ 1, 3, 5, 6 MHz, number of points in a trace: 505, 606, 1001.

Results are shown in Fig. 9, where dots represent the measured value and vertical segments the expanded uncertainty ($k = 2$). The horizontal dashed gray line represents the CP measured at each site, serving as the reference value to assess the significance of the proposed scalar MPE procedure. The expanded uncertainty interval ($k = 2$) is represented by the light gray strip.

A summary of ZS measurement is shown in Tab. 8, where $N_p$ is the number of points acquired in a trace, $N_T$ is the number of averaged traces for each acquisition in AVG mode, $n$ is the number of repeated measurements, $\hat{P}_{\text{traffic}}$ is the

**TABLE 8. Summary of ZS measurements.**

| Site | $N_p$ | SWT | RBW | $N_T$ | $n$ | $\hat{P}_{\text{traffic}}$ [nW] |
|---|---|---|---|---|---|---|
| Ivrea | 505 | 20 ms | 1 MHz | 100 | 2 | 184.87 ± 22.99 |
| | | | 3 MHz | | | 147.19 ± 7.03 |
| | | | 5 MHz | | | 119.32 ± 8.24 |
| | 606 | 20 ms | 1 MHz | 100 | 5 | 161.99 ± 9.85 |
| | | | 3 MHz | | 1 | 154.13 ± 6.47 |
| | | | 5 MHz | | 3 | 156.63 ± 26.70 |
| | 1001 | 20 ms | 1 MHz | 100 | 3 | 174.79 ± 8.79 |
| | | | 3 MHz | | | 96.89 ± 8.05 |
| | | | 5 MHz | | | 128.28 ± 12.80 |
| | | 33 ms | 6 MHz | | 1 | 101.26 ± 4.25 |
| | | | 3 MHz | 100 | 4 | 134.77 ± 7.01 |
| | | | 5 MHz | | 1 | 118.38 ± 4.97 |
| | | 40 ms | 1 MHz | 100 | 3 | 125.17 ± 8.95 |
| | | | 3 MHz | | 4 | 135.81 ± 6.10 |
| | | | 5 MHz | | 3 | 115.60 ± 5.36 |
| Rome | 1001 | 20 ms | 1 MHz | 1000 | 1 | 57.91 ± 5.34 |
| Turin | 505 | 20 ms | 5 MHz | 100 | 1 | 14.91 ± 2.20 |
| | 606 | 20 ms | 1 MHz | 100 | 1 | 13.62 ± 2.01 |
| | | | 3 MHz | | | 12.80 ± 1.89 |
| | | | 5 MHz | | 3 | 11.92 ± 1.91 |
| | 1001 | 20 ms | 5 MHz | 100 | 1 | 13.46 ± 1.99 |
| | | 33 ms | 1 MHz | 100 | 1 | 14.01 ± 2.07 |
| | | | 3 MHz | | | 14.58 ± 2.15 |
| | | | 5 MHz | | | 13.10 ± 1.94 |
| | | 40 ms | 5 MHz | 100 | 1 | 11.71 ± 1.73 |

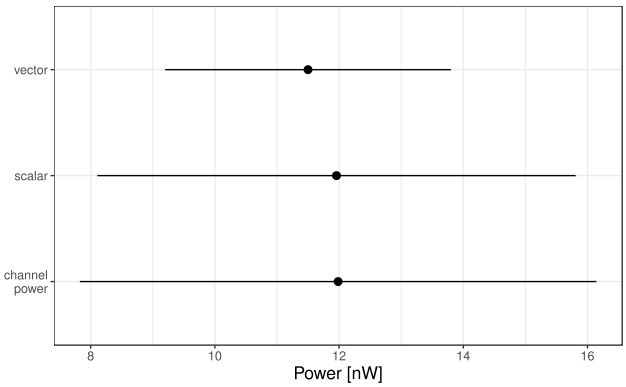


**FIGURE 10. Comparison of MPE values obtained from scalar, vector, and CP measurement in Turin.**

average value of $P_{\text{traffic}}$ with the associated uncertainty. Where repeated measurements were not available, only the $u_b$ contribution to the uncertainty given by the instrument could be evaluated resulting in a tighter uncertainty interval.

Fig. 9 shows generally a very good agreement between the scalar MPE values and the reference CP measurements: most uncertainty intervals of scalar and CP measurements overlap, even if in some cases (see for example the set of measurements for the Ivrea site) scalar measurements are at the lower bound of the CP uncertainty interval.

### D. A COMPARISON BETWEEN VECTOR AND SCALAR MEASUREMENT

As a last step, it is of interest to compare the vector and scalar methods. For a significant comparison, the two measurements methods had to be applied at the same time so that they operate on the same input signal. Therefore, in the measurement session in Turin a power splitter was inserted in the measurement chain to connect the same antenna to both the R&S FSW and the Keysight N9020 analyzers. In the previous Sections it was showed that the parameters setting tested in the various measurement sessions give results within the uncertainty range of the measurement.

For the comparison, the scalar method was applied with the following experimental configuration:

- SWT = 20 ms, equal to a multiple of the frame duration and to the SSB repetition period;
- number of points = 606, so that each time interval spanned by a pixel on the screen of the SA is very close to the symbol duration;
- RBW = 5 MHz, chosen because it is the largest value, that guarantees that a sufficiently large statistical sample of traffic REs is acquired,

while for the vector measurement the median $\tilde{x}$ of the measurement session was chosen (see the value $P_{\text{MPE}}$ (median) for "Turin afternoon" in Tab. 7). Furthermore, since the data forcing procedure allowed for a full use of the frame, CP measurements were also collected and used as direct estimation of the maximum power.

The results shown in Fig. 10 confirm that scalar and vector approach to MPE return comparable results (a $t$-test with $t = 0.14$ proves that they do not differ significantly, with $p < 0.01$), and that they are also in full agreement with the reference value provided by CP measurements.

With regards to the uncertainty associated with each method, the figure shows that it is lower for vector measurement than for the scalar and CP measurement. This is explained by the fact that the vector measurement is more precise because the analysis algorithm assures a perfect synchronization with the signal (as described in Appendix), which also relaxes the requirement for repeated measurement to assess the $u_a$ contribution to the uncertainty budget. On the contrary, repeatability is a significant contribution to uncertainty in the scalar approach, where synchronization is much less precise, and it is not possible to directly measure $P_{\text{PDSCH-RE,max}}$ (which is obtained by post-processing traces as shown in Sect. IV-C). For the CP measurement, uncertainty has been evaluated also taking into account the variation of the antenna factor within the bandwidth of the measured signal.

## V. CONCLUSION

In this paper, a novel MPE procedure for 5G systems, based on the direct measurement of the received power of traffic beams, is presented and experimentally validated. The technique takes advantage of a user terminal to force the traffic beam toward the measurement positions. In this way it is

possible to measure directly the power of the REs assigned to PDSCH.

The proposed procedure has a number of advantages:

1) it can be applied to both scalar or vector measurements;
2) it directly measures the quantity of interest for the MPE, i.e. the REs associated to the PDSCH channel transmitted by the traffic beam pointing toward the measurement point, thus avoiding the introduction of correction factors which tend to increase the overall uncertainty;
3) vector measurements are simple and do not require a uniformly full-loaded frame because it is possible to identify theREs associated to the traffic beam just observing the REs of the frame;
4) the multiple-acquisition procedure required by scalar measurements can be easily automatized.

Regarding the limitations, the ZS procedure proposed in this paper requires signal acquisition in average mode, therefore a uniformly full loaded frame is required during the acquisition time. This problem will be subject to further investigation.

## APPENDIX
## MEASUREMENT PROCEDURES
### A. VECTOR MEASUREMENTS

Although modern VSA are usually able to determine automatically all the parameters which characterize a 5G signal, this appendix describes in short each of the key steps needed to perform a successful vector analysis. In order to ensure a good synchronization with the 5G signal, a set of preliminary information about the investigated signal are needed:

- Spectral occupation and center frequency of the 5G signal;
- Center frequency of the SSB;
- Numerology;
- SSB Case;
- Cell ID.

All of the parameters listed above could be determined through experimental measurements. A short summary of how it could be done is provided in the following:

- **Preliminary spectrum overview**: first of all, a spectrum overview in N78 and N257 frequency bands is required to identify the spectrum regions where 5G NR signals can be detected. A MH trace setting with an RBW and Video Bandwidth (VBW) of some MHz is highly recommended due to the strong time variability exhibited by 5G NR signals;
- **Spectral occupation and center frequency of the 5G NR signal**: each spectrum band has to be investigated reducing progressively the span. A MH trace setting with a RBW and VBW of some hundreds of kHz allows to properly display the Orthogonal Frequency-Division Multiplexing (OFDM) spectrum of the signal and thus identify the spectral occupation and center frequency;
- **Center frequency of the SSB**: modern VSA can perform a real-time spectrum analysis (also known as waterfall spectrogram shown in Fig. 11). This analysis allows to highlight the region of the frequency spectrum which is characterized by the presence of a persistent, always-on SSB. Starting from a waterfall plot, it is easy to identify the offset between the 5G carrier frequency and the SSB center frequency;
- **Numerology**: real-time spectrum analysis also allows to determine the bandwidth $B_{\mathrm{SSB}}$ of the SSB. Since the SSB always spans 240 sub-carriers, the numerology can be trivially obtained with the formula: $\mu = B_{\mathrm{SSB}}/240$;
- **SSB Case**: VSA are usually equipped with 5G NR software analysis module which allows to display the time vs frequency grid of the signal. This grid allows to identify the position of the first symbol occupied by each SSB of a burst. This information, along with numerology, can be used to determine the SSB Case structure (A,B,C,D,E) [22, §4];
- **Cell ID**: once all the parameters discussed above are properly set, the VSA should be able to resolve the Cell IDs associated to the signal under investigation.

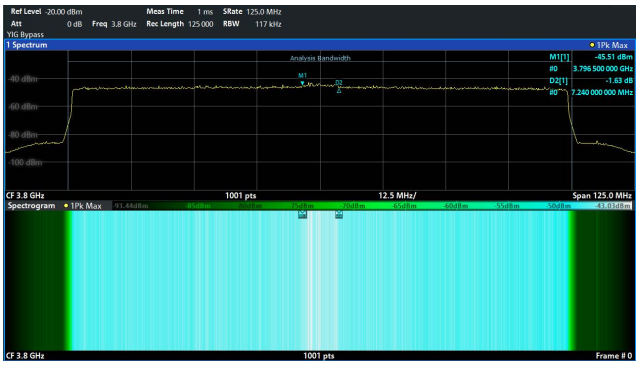


**FIGURE 11.** Determination of center frequency and bandwidth extension of the SSB by a waterfall spectrogram.

Although prior knowledge of the TDD configuration implemented by the 5G signal is not strictly required to perform a vector analysis of a 5G signal, the value of $F_{\mathrm{TDC}}$ parameter — i.e., the fraction of the signal frame reserved to downlink transmission [25] — is still required in order to apply eq. (2). A detailed description of the experimental procedure for the estimate of $F_{\mathrm{TDC}}$ can be found in [19].

Once the VSA shows a condition of full synchronization with the 5G signal, it is possible to force the traffic with a UE to obtain a full-loaded frame. Finally, a detailed analysis of the received power level per RE allows to infer the value of $P_{\mathrm{PDSCH\text{-}RE,max}}$ which could be used in eq. (2).

### B. SCALAR MEASUREMENTS

The measurement method developed on VSA is based on the following considerations:

- for the goals of this work, the frequency setting for the analysis in the time domain (ZS functionality of the analyzer) was chosen equal to that of the SSB center band;
- to verify the duplexing and measure the level of the SSBs and/or of traffic slots, it is necessary to synchronize the

analysis of the trace to the duration of the frame, and in particular to the repetition period of the SSBs. This synchronization was obtained using a periodic trigger, with a period equal to a multiple of the duration of the frame (10 ms), and a scan time set in such a way that the duration of the analysis of each pixel on the screen was close to the duration of a symbol (this indication derives from the provisions for 4G in [12]);

- in case of OFDM type signals with complex modulations, it is necessary to work with an RMS detector to avoid overestimating the read power (due to the high crest factor);
- the opening of the RBW filter was chosen lower than the SSB bandwidth occupation, in order to guarantee the proper detection both of the power level associated only with the control channels (not with any simultaneous and adjacent traffic channels in frequency), and the power level associated to traffic slots. In the measurement sessions of this work, depending on the characteristics of the power distribution in each frame, we could observe that greater repeatability is obtained when using values of RBW greater than 3 MHz, due to the greater number of samples from which the power level is measured, whereas greater variability can be seen when using an RBW of 1 MHz;
- again due to the OFDM signal with complex modulations, the VBW value was chosen greater than 3 times the width of the RBW filter;
- to obtain traffic slots amplitude, traces have to be acquired in AVG mode. In this work, an average on 100 traces was chosen. For this type of measurement, it is important to assure, through adequate traffic-forcing, that the full-frame condition is maintained during the acquisition of the entire set of 100 traces.

After acquiring the traces obtained with the above described criteria, the traffic slots power level can be determined by analyzing the density function of the trace pixels, by calculating the mode of the distribution.

Eventually, the power per RE has to be calculated, by correcting the obtained power value for the ratio between subcarrier spacing and noise bandwidth.

## REFERENCES

[1] S. Adda, T. Aureli, S. Coltellacci, S. D'Elia, D. Franci, E. Grillo, N. Pasquino, S. Pavoncello, R. Suman, and M. Vaccarono, "A methodology to characterize power control systems for limiting exposure to electromagnetic fields generated by massive mimo antennas," *IEEE Access*, vol. 8, pp. 171956–171967, 2020.

[2] P. Baracca, A. Weber, T. Wild, and C. Grangeat, "A statistical approach for RF exposure compliance boundary assessment in massive MIMO systems," in *Proc. 22nd Int. ITG Workshop Smart Antennas (WSA)*, 2018, pp. 1–6.

[3] K. Bechta, C. Grangeat, and J. Du, "Impact of effective antenna pattern on radio frequency exposure evaluation for 5G base station with directional antennas," in *Proc. XXXIII Gen. Assem. Sci. Symp. Int. Union Radio Sci.*, 2018, pp. 1–4.

[4] B. Thors, A. Furuskär, D. Colombi, and C. Törnevik, "Time-averaged realistic maximum power levels for the assessment of radio frequency exposure for 5G radio base stations using massive MIMO," *IEEE Access*, vol. 5, pp. 19711–19719, 2017.

[5] D. Pinchera, M. Migliore, and F. Schettino, "Compliance boundaries of 5G massive MIMO radio base stations: A statistical approach," *IEEE Access*, vol. 8, pp. 182787–182800, 2020.

[6] D. Colombi, P. Joshi, B. Xu, F. Ghasemifard, V. Narasaraju, and C. Törnevik, "Analysis of the actual power and EMF exposure from base stations in a commercial 5G network," *Appl. Sci.*, vol. 10, no. 15, p. 5280, Jul. 2020.

[7] S. Aerts, L. Verloock, M. Van den Bossche, D. Colombi, L. Martens, C. Tornevik, and W. Joseph, "Design and validation of an *in-situ* measurement procedure for 5G NR base station RF-EMF exposure," in *Proc. Joint Annu. Meeting Bioelectromag. Soc. Eur. BioElectromag. Assoc. (BioEM)*, 2020, pp. 414–418.

[8] C. Bornkessel, T. Kopacz, A.-M. Schiffarth, D. Heberling, and M. A. Hein, "Determination of instantaneous and maximal human exposure to 5G massive-MIMO base stations," in *Proc. 15th Eur. Conf. Antennas Propag. (EuCAP)*, Mar. 2021, pp. 1–5.

[9] M. D. Migliore and F. Schettino, "Power reduction estimation of 5G active antenna systems for human exposure assessment in realistic scenarios," *IEEE Access*, vol. 8, pp. 220095–220107, 2020.

[10] A. Hirata, Y. Diao, T. Onishi, K. Sasaki, S. Ahn, D. Colombi, V. De Santis, I. Laakso, L. Giaccone, J. Wout, E. Rashed, W. Kainz, and J. Chen, "Assessment of human exposure to electromagnetic fields: Review and future directions," *IEEE Trans. Electromagn. Compat.*, vol. 63, no. 5, pp. 1619–1630, Oct. 2021.

[11] S. Adda, T. Aureli, S. D'Elia, D. Franci, E. Grillo, M. D. Migliore, S. Pavoncello, F. Schettino, and R. Suman, "A theoretical and experimental investigation on the measurement of the electromagnetic field level radiated by 5G base stations," *IEEE Access*, vol. 8, pp. 101448–101463, 2020.

[12] *Determination of RF Field Strength, Power Density and SAR in the Vicinity of Radiocommunication Base Stations for the Purpose of Evaluating Human Exposure*, Standard IEC 62232, International Electrotechnical Commission, 2017.

[13] S. Aerts, K. Deprez, D. Colombi, M. Van den Bossche, L. Verloock, L. Martens, C. Törnevik, and W. Joseph, "*In situ* assessment of 5G NR massive MIMO base station exposure in a commercial network in Bern, Switzerland," *Appl. Sci.*, vol. 11, no. 8, p. 3592, Apr. 2021.

[14] N. Pasquino and R. S. L. Moriello, "A critical note to the standard procedure for assessing exposure to GSM electromagnetic field," *Measurement*, vol. 73, pp. 563–575, Sep. 2015.

[15] N. Pasquino, "Measurement and analysis of human exposure to electromagnetic fields in the GSM band," *Measurement*, vol. 109, pp. 373–383, Oct. 2017.

[16] H. Keller, "On the assessment of human exposure to electromagnetic fields transmitted by 5G NR base stations," *Health Phys.*, vol. 117, no. 5, pp. 541–545, Nov. 2019.

[17] S. Aerts, L. Verloock, M. Van Den Bossche, D. Colombi, L. Martens, C. Törnevik, and W. Joseph, "*In-situ* measurement methodology for the assessment of 5G NR massive MIMO base station exposure at sub-6 GHz frequencies," *IEEE Access*, vol. 7, pp. 184658–184667, 2019.

[18] D. Franci, S. Coltellacci, E. Grillo, S. Pavoncello, T. Aureli, R. Cintoli, and M. D. Migliore, "Experimental procedure for fifth generation (5G) electromagnetic field (EMF) measurement and maximum power extrapolation for human exposure assessment," *Environments*, vol. 7, no. 3, p. 22, Mar. 2020.

[19] D. Franci, S. Coltellacci, E. Grillo, S. Pavoncello, T. Aureli, R. Cintoli, and M. D. Migliore, "An experimental investigation on the impact of duplexing and beamforming techniques in field measurements of 5G signals," *Electronics*, vol. 9, no. 2, p. 223, Jan. 2020.

[20] T. Kopacz, S. Schießl, A.-M. Schiffarth, and D. Heberling, "Effective SSB beam radiation pattern for RF-EMF maximum exposure assessment to 5G base stations using massive MIMO antennas," in *Proc. 15th Eur. Conf. Antennas Propag. (EuCAP)*, Mar. 2021, pp. 1–5.

[21] A.-K. Lee, S.-B. Jeon, and H.-D. Choi, "EMF levels in 5G new radio environment in Seoul, Korea," *IEEE Access*, vol. 9, pp. 19716–19722, 2021.

[22] *NR; Physical Layer Procedures for Control*, document TS 38.213, Revision 15.1.0, 3rd Generation Partnership Project (3GPP), Apr. 2018.

[23] M. D. Migliore, D. Franci, S. Pavoncello, E. Grillo, T. Aureli, S. Adda, R. Suman, S. D'Elia, and F. Schettino, "A new paradigm in 5G maximum power extrapolation for human exposure assessment: Forcing gNB traffic toward the measurement equipment," *IEEE Access*, vol. 9, pp. 101946–101958, 2021.

[24] *R: A Language and Environment for Statistical Computing*, R Core Team, R Found. Stat. Comput., Vienna, Austria, 2021. [Online]. Available: https://www.R-project.org/

[25] *Case Studies Supporting IEC 62232—Determination of RF Field Strength, Power Density and SAR in the Vicinity of Radiocommunication Base Stations for the Purpose of Evaluating Human Exposure*, Standard IEC-TR 62669, International Electrotechnical Commission, 2019.

**SARA ADDA** received the M.Sc. degree *(cum laude)* in physics and the postgraduate specialization degree in health physics from Turin University, Italy, in 1998 and 2003, respectively.

She worked for one year (1998–1999) at ENEA Casaccia, Rome, within the Interdepartmental Computing and High Performance Networks Project, implementing a system for the simulation of electromagnetic field dynamics in complex environments through the use of massively parallel architectures. Since 1999, she has been working at the Physical and Technological Risk Department, ARPA Piedmont, dealing with control and monitoring of non-ionizing radiation and the development of theoretical forecasting/numerical calculation methods, both in the low and high frequency ranges. She also participates in the Italian Electrotechnical Committee (CEI) working groups, for the drafting of technical standards on measurement and evaluation methods for human emf exposure and she deals with the theoretical and practical aspects related to the measurement of electromagnetic fields in the workplace. In this context, she is the Representative of the Interregional Technical Coordination Group of the Piedmont Region. She participates in European (Twinning Italy–Poland project) and international collaborative projects (Arpa Piemonte—Beijing Municipal Environmental Protection Bureau), on methods and techniques for measuring and evaluating human exposure to emf both in the workplace and in the living environment.

**TOMMASO AURELI** received the M.Sc. degree in biological science from Sapienza University, Rome, Italy, in 1985. He joined ARPA Lazio, in 2002. From 2004 to 2018, he was the Director of the EMF Division, being involved in both measurement and previsional evaluation of EMF from civil sources. He is currently the Director of the Department of Rome.

**SERGIO BASTONERO** received the degree in electronic engineering and the Ph.D. degree in electronic and communications engineering from the Politecnico di Torino, Turin, Italy, in 1995 and 2000, respectively. Since 1999, he has been working at CSELT—Centro Studi E Laboratori Telecomunicazioni, now Telecom Italia (TIM). He has contributed to the development of tools for verifying and certifying the compliance of radio-base-stations to electromagnetic exposure. He has also contributed to the drafting of international standards for the characterization of active and passive antennas for radio-base stations.

**STEFANO D'ELIA** received the M.Sc. degree *(magna cum laude)* in electronics engineering from the University of Rome "La Sapienza," in 1997.

He joined Vodafone, formerly Omnitel, in 1998, where he is currently covering the role of Mobile Access Integrated Solutions Manager at Vodafone Networks, based in Ivrea, Turin, Italy. His main professional interests include energy efficiency modeling for mobile networks and calculation and measurements for the assessment of human exposure to high-frequency electromagnetic fields from mobile base stations.

Dr. D'Elia has been the National Delegate in several standard bodies on electromagnetic fields measurements and calculations. In 2012, he was awarded as a Vodafone Distinguished Engineer, one of the highest steps in the technical career path at Vodafone. Since 2002, he has been the Appointed Chairperson of the Working Group "Mobile Base Stations and IoT" within the Technical Committee 106 "Human exposure to electromagnetic fields" of the Italian Electrotechnical Committee.

**DANIELE FRANCI** received the M.Sc. *(magna cum laude)* and Ph.D. degrees in nuclear and subnuclear physics from Sapienza University, Rome, Italy, in 2007 and 2011, respectively. From 2009 to 2011, he was an Analyst Technologist with Nucleco S.P.A., involved in radiological characterization of radioactive wastes from the decommissioning of former Italian nuclear power plants. He joined ARPA Lazio, in 2011, being involved in RF EMF human exposure assessment. Since 2017, he has been involved in activities of CEI for the definition of technical procedures for EMF measurement from 4G/5G MIMO sources.

**ENRICO GRILLO** received the M.Sc. degree in electronics engineering from the Seconda Università di Napoli, Aversa, Italy, in 1999. In 2000, he worked as a RF to grow up the first 3G telecommunication radio network. Since 2005, he has been involving as a Research Technician in prevention and monitoring of electromagnetic pollution at ARPA Lazio, the local environmental agency of the Lazio Region.

**MARCO DONALD MIGLIORE** (Senior Member, IEEE) received the Laurea (Hons.) and Ph.D. degrees in electronic engineering from the University of Naples, Naples, Italy.

He was a Visiting Professor at the University of California at San Diego, La Jolla, CA, USA, in 2007, 2008, and 2017, the University of Rennes I, Rennes, France, in 2014 and 2016, the Centria Research Center, Ylivienka, Finland, in 2017, the University of Brasilia, Brazil, in 2018, and the Harbin Technical University, China, in 2019. He is currently a Full Professor at the University of Cassino and Southern Lazio, Cassino, Italy, where he is also the Head of the Microwave Laboratory and the Director of studies of the ITC courses. He is a member of the ELEDIA@UniCAS Research Laboratory, ICEMmB—National Interuniversity Research Center on the Interactions Between Electromagnetic Fields and Biosystems, where he is the Leader of 5G group at the Italian Electromagnetic Society (SIEM) and the National Interuniversity Consortium for Telecommunication (CNIT). He was a Speaker at the Summer Research Lecture Series of the UCSD CALIT2 Advanced Network Science, in 2008. His current research interests include the connections between electromagnetism and information theory, the analysis, synthesis, and characterization of antennas in complex environments, antennas and propagation for 5G and beyond, measurement techniques for the assessment of human exposure to 5G, compressed sensing as applied to electromagnetic problems, and energetic applications of microwaves. He serves as a referee for many scientific journals and has served as an Associate Editor for IEEE TRANSACTIONS ON ANTENNAS AND PROPAGATION.

**NICOLA PASQUINO** (Senior Member, IEEE) was born in Naples, Italy, in 1973. He received the M.Sc. degree *(magna cum laude)* in electronics engineering and the Ph.D. degree in information engineering from the Università degli Studi di Napoli Federico II, Naples, in 1998 and 2002, respectively.

He was a Fulbright Scholar at the University of Pennsylvania, Philadelphia, PA, USA, in 2000–2001. He is currently a Professor of Electrical and Electronic Measurements at the Department of Electrical Engineering and Information Technologies, Università degli Studi di Napoli Federico II. He is the Chief Scientist at the Electromagnetic Compatibility Laboratory, Department of Electrical Engineering and Information Technologies. His research interests include electromagnetic compatibility measurements and measurements of human exposure to high-frequency electromagnetic fields, with application of machine learning methodologies to measurement data analysis.

Prof. Pasquino was the President of Rotary Club Napoli Angioino (D2101, Italy), in 2019–2020. He has been a member of Rotary, since 2005. He is the President of the TC106 "Human exposure to electromagnetic fields" of the Italian Electrotechnical Committee. He is also the Convenor of the Committee "Human exposure to electromagnetic fields" within the Engineering Register of Naples. He is a member of the Editorial Board for the *Measurement Science Review* journal. He serves as an Editor for the *Journal of Electrical and Computer Engineering* and a Section Editor for the *Acta IMEKO* journal.

**SETTIMIO PAVONCELLO** was born in Rome, Italy, in 1973. He received the M.Sc. degree in telecommunication engineering from the Sapienza University of Rome, Italy, in 2001. Since 2002, he has been working at the Regional Environmental Agency of Lazio, Rome EMF Department. He is specialized in electromagnetic field measurements and EMF projects evaluation related to radio, TV, and mobile communications systems maturing huge experience in the use of broadband and selective instruments. In last years, he has deepened the issues related to measurements on LTE and NB-IoT signals. Since 2018, he has been actively involving at the Working Group "Mobile Base Stations" within the Technical Committee 106 of the Italian Electrotechnical Committee (CEI) aimed at defining measurement procedures for mobile communications signals and is currently engaged in various projects concerning measurement on 5G signals.

**FULVIO SCHETTINO** (Senior Member, IEEE) received the Laurea (Hons.) and Ph.D. degrees in electronic engineering from the University of Naples, Naples, Italy. He is currently an Associate Professor at the University of Cassino and Southern Lazio, Cassino, Italy. He is a member of the ELEDIA@UniCAS Research Laboratory, ICEMmB—National Interuniversity Research Center on the Interactions Between Electromagnetic Fields and Biosystems, the Italian Electromagnetic Society (SIEM), and the National Interuniversity Consortium for Telecommunication (CNIT). His current research interests include numerical electromagnetics, regularization methods, the connections between electromagnetism and information theory, the analysis, synthesis, and characterization of antennas in complex environments, antennas and propagation for 5G, and energetic applications of microwaves.

**ANDREA SCHIAVONI** (Member, IEEE) received the degree in electronic engineering and the Ph.D. degree in electromagnetic compatibility from the University of Ancona, Italy, in 1990 and 1994, respectively. In 1993, he joined CSELT—Centro Studi E Laboratori Telecomunicazioni. Since the beginning, he has been involving in computational electrodynamics and measurement activities relevant to human exposure to electromagnetic fields from cellular phones. He has developed and got accreditation of the SAR Laboratory in CSELT and then TIM. From 2002 to 2008, he was responsible for radio testing of user equipment, including OTA and SAR. Since 2012, he has been involving in radio planning and exposure to electromagnetic fields from base stations. He is a member of CEI CT106, IEC TC106, and IEEE TC34. He was the Co-Chair of IEEE P1528.7 "IEEE Guide for EMF Exposure Assessment of the Internet of Things (IoT) Technologies and Devices."

**RENATO SCOTTI** received the degree in telecommunication engineering from the Politecnico di Torino, Italy, in 2001. He joined TILab—Telecom Italia Lab, now TIM, in 2002. He worked on far-to-near field transformation algorithms specific for radio base station antennas, development of active antennas prototypes in collaboration with manufacturers, and validation of algorithms and methodologies for electromagnetic fields (EMF) monitoring. He is currently involved in the development of the EMF framework that TIM adopts for the EMF exposure assessment to ensure the compliance of its radio base stations to the Italian legislation on human exposure. He collaborates with CEI CT106 on these issues.

**RICCARDO SUMAN** was born in Ivrea, Italy, in 1974. He received the B.Sc. degree in telecommunication engineering from the Politecnico di Torino, Italy, in 1996. Since 1996, he has been with Vodafone (formerly Omnitel Pronto Italia), where he is currently working as an Antenna Subject Matter Expert. He also participates at the BASTA AA (Recommendation on Base Station Active Antenna Standards) by NGMN Alliance. Since 2012, he has been involved in activities related to EMF focusing on measuring and modeling electromagnetic fields and electromagnetic exposure assessment of base stations for mobile communications. He also participates at the Technical Committee 106 of the Italian Electro Technical Committee (CEI) and the National Delegate to the IEC TC106.

**MATTIA VACCARONO** was born in Ivrea, Italy, in 1990. He received the M.Sc. degree *(magna cum laude)* in physics from Turin University, in 2015. He is currently pursuing the Ph.D. degree with the Electrical and Computer Engineering Department, Colorado State University, conducting research on weather radars and EMF interference. Since 2016, he has been working at the Regional Agency for Environmental Protection (Arpa Piemonte) of Piedmont Region, Italy. He is specialized in EMF measurements and project assessments.